The Journal of Infectious Diseases

MAJOR ARTICLE

Experimental Infection of Syrian Hamsters With Aerosolized Nipah Virus

Olivier Escaffre,[1] Terence Hill,[1] Tetsuro Ikegami,[1,2,3] Terry L. Juelich,[1] Jennifer K. Smith,[1] Lihong Zhang,[1] David E. Perez,[1] Colm Atkins,[1] Arnold Park,[5] William S. Lawrence,[4] Satheesh K. Sivasubramani,[4] Jennifer E. Peel,[4] Johnny W. Peterson,[3,4] Benhur Lee,[6] and Alexander N. Freiberg[1,2,3]

[1]Department of Pathology, [2]Center for Biodefense and Emerging Infectious Diseases, [3]Institute for Human Infections and Immunity, and [4]Department of Microbiology and Immunology, University of Texas Medical Branch, Galveston; [5]Department of Pathology and Immunology, Washington University School of Medicine, St Louis, Missouri; and [6]Department of Microbiology, Icahn School of Medicine at Mount Sinai, New York, New York

Background. Nipah virus (NiV) is a paramyxovirus (genus *Henipavirus*) that can cause severe respiratory illness and encephalitis in humans. Transmission occurs through consumption of NiV-contaminated foods, and contact with NiV-infected animals or human body fluids. However, it is unclear whether aerosols derived from aforesaid sources or others also contribute to transmission, and current knowledge on NiV-induced pathogenicity after small-particle aerosol exposure is still limited.

Methods. Infectivity, pathogenicity, and real-time dissemination of aerosolized NiV in Syrian hamsters was evaluated using NiV-Malaysia (NiV-M) and/or its recombinant expressing firefly luciferase (rNiV-Fluc^{NP}).

Results. Both viruses had an equivalent pathogenicity in hamsters, which developed respiratory and neurological symptoms of disease, similar to using intranasal route, with no direct correlations to the dose. We showed that virus replication was predominantly initiated in the lower respiratory tract and, although delayed, also intensely in the oronasal cavity and possibly the brain, with gradual increase of signal in these regions until at least day 5–6 postinfection.

Conclusion. Hamsters infected with small-particle aerosolized NiV undergo similar clinical manifestations of the disease as previously described using liquid inoculum, and exhibit histopathological lesions consistent with NiV patient reports. NiV droplets could therefore play a role in transmission by close contact.

Keywords. aerosol; animal model; hamster; henipavirus; Nipah virus; pathogenesis; in vivo imaging.

Nipah virus (NiV) is a fruit bat-borne, emerging paramyxovirus that can cause severe respiratory illness and encephalitis in humans and livestock (cattle, pigs, and goats) [1–3]. The case fatality rate is estimated at 40% to 75%; however, this rate can vary depending on the size of the outbreak. Currently, there are no approved vaccines or therapeutics available for human use. The first NiV-infected patients were reported during a large outbreak among swine abattoir workers and pork merchants in Malaysia and Singapore in 1998–1999 [2, 4–6]. Sporadic outbreaks have been identified yearly in Bangladesh and India since 2001, and stem from residents consuming NiV-contaminated food, with subsequent human-to-human spread among hospital personnel and family members of the patient [7–12]. Histopathological analyses on fatal cases of patients from the Malaysia outbreak are the only available and describe a viral tropism for multiple organs during the terminal stage of the disease [3]. However, the lack of data from patients exhibiting early clinical symptoms of infection hampers a complete understanding of a natural human NiV infection, as well as how NiV disseminates in patients. Several NiV infection animal models, including Syrian hamsters, have shown that an intranasal route—a presumed route for a natural human infection—leads to the development of a neurological and respiratory disease [13–19], as seen with NiV-infected patients [1, 4, 5, 9, 11, 20–24]. Additionally, the upper and lower respiratory tract epithelium was recently reported as an early target of infection in the hamster model [25] as well as permissive to replication in human in vitro model systems [26, 27].

Close respiratory contact with NiV-infected animals, NiV-contaminated human respiratory secretions, or body fluids was suspected to be the mode of transmission [4–7, 12, 24], in addition to NiV-contaminated food [23, 28], suggesting that NiV can also spread by aerosol in the form of droplets that travel short distances. This corroborates the data from a recent study describing the first small-particle NiV-Malaysia (NiV-M) aerosol infection in the African green monkey (AGM) model, where animals developed a severe respiratory disease [29]. Here, the objective was to characterize the pathogenicity of aerosolized NiV in the Syrian hamster model. This model is one of the most relevant and well-characterized rodent models to study NiV pathogenesis, as well as to evaluate vaccines and antivirals, because it encompasses the major aspects of clinical disease seen in patients [15, 16, 18, 19, 25, 30]. We showed that small-particle aerosolized NiV-M and recombinant NiV-M encoding firefly

Received 14 February 2018; editorial decision 7 June 2018; accepted 12 June 2018; published online June 15, 2018.

Correspondence: A. N. Freiberg, PhD, Department of Pathology, University of Texas Medical Branch, 301 University Boulevard, Galveston, Texas 77555-0609 (anfreibe@utmb.edu).

The Journal of Infectious Diseases® 2018;218:1602–10

DOI: 10.1093/infdis/jiy357

luciferase (rNiV-Fluc^{NP}) [31] had a comparable median lethal dose, and induced clinical signs of respiratory and neurological disease irrespective of the dose. A trend of increasing incidence in respiratory signs with increasing dose of the recombinant virus was, however, noted. Tropism of both small-particle aerosolized viruses was also similar, although rNiV-Fluc^{NP}-induced lesions in the lungs were less frequent. Using an in vivo imaging system (IVIS), we finally showed that replication of aerosolized rNiV-Fluc^{NP} was initially primarily confined to the lungs, and then also intensely found in the oronasal cavity and possibly brain area, starting day 2–3 postinfection.

MATERIAL AND METHODS

Ethics Statement

Animal experiments were approved by the Institutional Animal Care and Use Committee of the University of Texas Medical Branch (UTMB) and performed following the guidelines of the Association for Assessment and Accreditation of Laboratory Animal Care International (AAALAC) by certified staff in an AAALAC-approved facility.

Viruses

Nipah virus (199901924 Malaysia prototype strain; NiV-M) used in this study had been passaged a total of 6 times in VeroE6 (ATCC, CRL1586) cells. Recombinant Nipah virus expressing firefly luciferase (rNiV-Fluc^{NP}) was constructed as previously described [31]. Virus titers were determined by plaque assay on Vero cells (ATCC, CCL-81) as previously described [31]. All work with infectious virus was performed under Biosafety Level 4 (BSL-4) conditions in the Robert E. Shope, MD, and the Galveston National Laboratory at UTMB.

Aerosol Exposure and Monitoring of Animals

Four- to 5-week-old female Syrian hamsters were obtained from Harlan Laboratories. Animals were housed in microisolator cages (n = 5 hamsters per cage). Groups of 5 unanesthetized hamsters were exposed to aerosol target doses ranging from 10^1 to 10^5 per hamster of Nipah virus (NiV-M and rNiV-Fluc^{NP}, respectively) for 15 minutes in the BSL-4 aerobiology suite using an automated Biaera aerosol system with whole-body aerosol chamber. During challenge, the animals were placed in stainless steel perforated boxes, which were then placed inside the aerosol chamber. A 3-jet Collison nebulizer (Mesa labs) was utilized to generate the aerosol in the chamber. Integrated air samples were obtained during exposures using a BioSampler (SKC Inc.). Cell culture medium (Dulbecco's Modified Eagle's Medium plus 2% fetal bovine serum plus 20 µL of antifoam) was used as a collection medium in the BioSampler. The presented dose (D_p), which denoted the number of plaque forming units (PFU) inhaled into the lungs of the animals, was determined as described by Roy and Pitt [32]. Briefly, $Dp = C_{AERO} \times MV \times T_{EXP}$, where C_{AERO} is the aerosol concentration in the exposure chamber, *MV* is the respiratory minute volume, and T_{EXP} is the total exposure time. The *MV* for hamsters were determined using Guyton's formula [33], which is based on the animals' weight. The estimated *MV* ranged between 54.81 and 58.30 mL/min. Plaque assays were done using mycoplasma-negative Vero-E6 cells for enumerating virus in the air samples collected during the exposure.

Animals were monitored daily for the development of clinical signs of disease and changes in body weight. Animals demonstrating a >20% body weight loss, paralysis, and/or gasping for air were humanely euthanized. The criteria of respiratory disease involvement were any change in breathing (labored, irregular) and a bloody nose. Criteria of a neurological involvement included aggressive behavior, any form of paralysis (rear, front), ataxia, head tilt, and seizure. Each of these criteria were counted as 1 score unit and tabulated per group so as to investigate any correlation with dose and respiratory or neurological disease. The maximum score for respiratory and neurological clinical signs was 2 or 5 per animal, respectively, with 5 animals per group.

In Vivo Imaging

For in vivo bioluminescence imaging (IVIS) at BSL-4 containment, hamsters were shaved to maximize detection of bioluminescent signals resulting from infection with rNiV-Fluc^{NP}. Prior to imaging, hamsters were anesthetized with 2% isoflurane and inoculated with D-luciferin (Caliper) via the intraperitoneal route (150 mg/kg). Bioluminescence was measured using an IVIS Spectrum platform (Perkin Elmer), which was equipped with a charge-coupled device camera system. Images were analyzed with the Living Image 4.3.1 software package. Acquisition time was set to auto for each image, with fixed f/stop at F1, and medium binning.

Tissue Histology

Necropsies were performed on euthanized animals, and lungs, spleens, and brains were collected for histopathology and immunohistochemistry. Tissues were immersion-fixed in 10% neutral buffered formalin for at least 4 days under BSL-4 conditions with regular formalin changes. Specimens were then processed under BSL-2 conditions. Briefly, tissues were dehydrated through a series of graded ethanol baths, infiltrated by and embedded with paraffin wax, sectioned at 5 µm thickness, and stained with hematoxylin and eosin. Immunohistochemistry for NiV nucleoprotein detection was performed using a rabbit anti-NiV-nucleoprotein antibody incubated overnight (kindly provided by Dr C. Broder, Uniformed Services University, Bethesda, Maryland) and a secondary horseradish peroxidase (HRP)-conjugated goat antirabbit antibody (Abcam) incubated for 2 hours (both 1:1000). DAB substrate (ThermoScientific) was then added for 2 minutes to enable chromogenic detection (brown precipitate) of HRP activity.

Statistical Analysis

Statistical analysis was performed with GraphPad Prism (GraphPad Software). The *t* test and Pearson *R* correlation test

were used to compare the mean time to death data (*$P < .05$, **$P < .01$) or to assess correlation between dose and clinical symptoms, respectively.

RESULTS

Survival and Clinical Observations in Hamsters After Aerosol Exposure to NiV-M and rNiV-Fluc^{NP}

The goal of this study was to characterize the pathogenicity of aerosolized Nipah virus in the Syrian hamster model, and to monitor virus spread by applying in vivo imaging. Initially, we attempted to determine the mean lethal dose (LD_{50}) for wild-type NiV-M and rNiV-Fluc^{NP} [31]. In an initial experiment, groups of 5 hamsters were exposed via whole-body aerosol to 4 different NiV-M doses ranging from 10^2 to 10^5 PFU/animal. Based on the calculated presented doses (Dp) (Figure 1A), the LD_{50} value was estimated to be lower than 10^2 PFU in hamsters (Figure 1A). From this result, we then performed a second similar aerosol exposure study using 5 different rNiV-Fluc^{NP} doses ranging from 10^1 to 10^5 PFU/animal (Figure 1B). The LD_{50} value was estimated to be lower than 10^1 PFU in hamsters.

Hamsters exposed to wild-type NiV-M began to lose body weight by day 5 postinfection (Figure 1C) and succumbed to disease or were euthanized between days 6 and 14 postinfection. The back titration of the inocula matched the targeted doses (Figure 1A), based on the acceptable variability range for the assay. Interestingly, 2/5 hamsters (40%) in each group exhibited both respiratory and neurological symptoms, and the remaining 3/5 (60%) animals from the 10^2, 10^3, and 10^4 PFU dose groups exhibited only neurological symptoms. The 3/5 (60%) remaining subjects from the 10^5 PFU dose group quickly succumbed to infection without developing symptoms other than weight loss and scruffy coat. Overall, no correlation was established between dose and respiratory or neurological clinical signs of disease, because both appeared first in some animals at the highest dose group as early as day 6. The mean time to death (MTD) in the 10^5 PFU dose group of animals was 7.2 days, and was shorter than in those animal groups challenged with 10^4 PFU (10.6 days; $P < .05$), 10^3 PFU (11.8 days; $P < .05$), and 10^2 PFU (13.5 days; $P < .01$) PFU.

Disease progression in hamsters infected with rNiV-Fluc^{NP} appeared similar to that in animals challenged with wild-type NiV-M. Hamsters succumbed to disease or were euthanized between day 6 and 15 postinfection (Figure 1D), although 2 hamsters (40%) in each 10^1 and 10^2 PFU dose group only transiently displayed a scruffy coat or weight loss. The back titration of the inocula matched the Dp (Figure 1B), based on the acceptable variability range for the assay, except in the 10^3 and 10^4 PFU dose groups, which were delivered at higher doses of 9.5×10^3 and 8.5×10^4 PFU, respectively. As the highest delivered dose was still higher than the latter, the groups of 5 animals per dose were maintained in order to compare with the data from the NiV-M groups. Similar to infections with wild-type NiV-M, 2 to 4 out of 5 hamsters (40% to 80%) in the 10^1, 10^2, 10^3, and 10^4 PFU dose

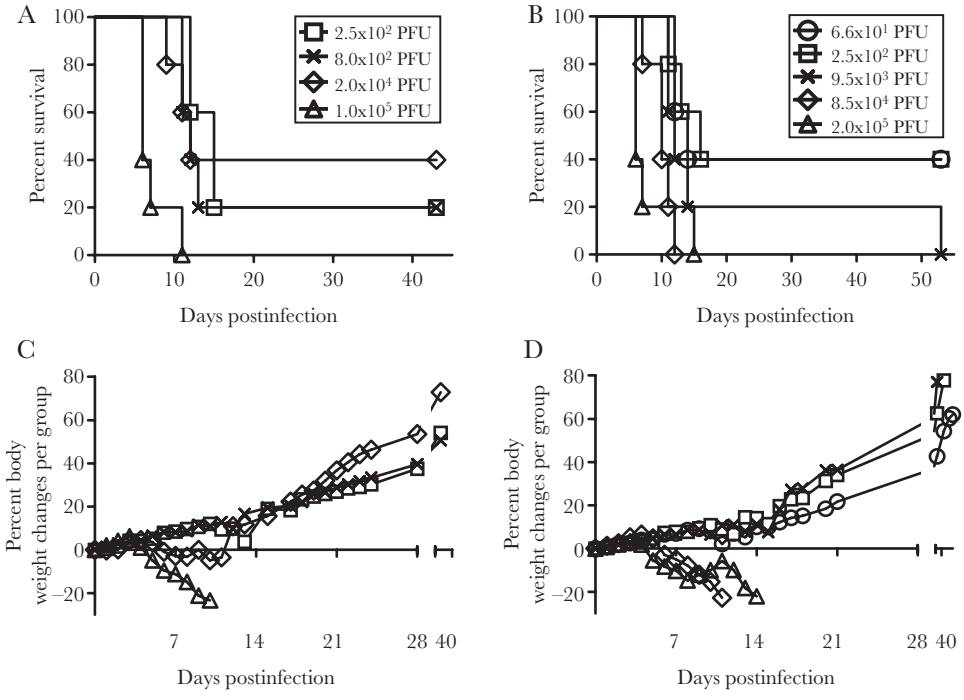

Figure 1. Susceptibility of Syrian hamsters to aerosol exposure with Nipah virus Malaysia strain (NiV-M) and recombinant Nipah virus (rNiV-Fluc^{NP}). Survival analysis of hamsters (n = 5 per group) exposed to (*A*) 10^2–10^5 PFU of NiV-M or (*B*) 10^1–10^5 PFU of rNiV-Fluc^{NP}. Body weight changes of (*C*) NiV-M–infected and (*D*) rNiV-Fluc^{NP}–infected hamsters in different groups monitored for 43 and 55 days postinfection, respectively. Abbreviation: PFU, plaque forming unit.

groups exhibited both respiratory and neurological symptoms, without any correlation to viral dose. All other subjects with symptoms beyond weight loss, except one from the 10^3 PFU dose group, presented with respiratory symptoms only. From the 10^5 PFU dose group, 4 hamsters (80%) rapidly succumbed to infection after only exhibiting weight loss, scruffy coat, and labored breathing, while the last animal (20%) displayed both neurological and respiratory symptoms, and succumbed later to infection. Altogether, no correlation between dose and respiratory or neurological symptoms of disease could be established, although a trend in increase of the respiratory symptoms incidence with the dose was noticed, and also both respiratory and neurological symptoms appeared first in some animals from the 2 highest dose groups at day 6 or 8 postinfection, respectively. Similar to infections with wild-type NiV-M, the MTD in the 10^5 PFU dose group was 8 days, and was shorter than in 10^4 (10 days; $P < .05$), 10^3 (12 days; $P < .05$), 10^2 (13.3 days; $P < .05$), and 10^1 (12.7 days; $P < .05$) PFU dose groups. Therefore, our data indicated that rNiV-Fluc^{NP} was not attenuated in hamsters in comparison to NiV-M after small-particle aerosol exposure.

Pathological Features in Hamsters After Aerosol Exposure to NiV-M and rNiV-Fluc^{NP}

Macroscopic observations of the lungs showed multifocal areas of hemorrhage, as well as nodules resembling abscesses or tissue necrosis, and whose presence across the lobes increased with the infective dose (data not shown).

Histopathological lesions and virus spread analysis was performed on tissues from 5 hamsters, pooled from animals in the 10^4 and 10^5 PFU dose groups, with respiratory and neurological clinical signs (Table 1), and that were euthanized within the same time frame as animals from lower-dose groups. NiV-M–induced lesions in the lung covered large areas of the bronchiolar interstitium and were characterized by frequent hyperplasia of type II pneumocytes (Figure 2A) and multinucleated giant cells appearing in the alveoli (Table 1) coinciding with the presence of viral antigen (data not shown). Any of the following lesions were also reported in at least 60% (3/5) of hamsters: vasculitis of medium to large blood vessels where NiV antigen was found (Figure 2B), edema, and presence of immune cells in alveoli (Table 1). Lungs from the two 10^5 PFU dose group animals featured additional lesions, such as frequent hemorrhages in alveoli, as well as rare to frequent thrombi formation. The rNiV-Fluc^{NP}–induced lesions were found in the bronchiolar interstitium but were rare, and also included multinucleated giant cells, edema, hemorrhage in alveoli, and thrombosis. Interestingly, the lung tissues from hamsters of the 10^5 PFU dose group only showed lesions of the respiratory epithelium (Table 1). Overall, 80% (4/5) of NiV-M or rNiV-Fluc^{NP}-infected hamsters exhibited a mild meningitis but with variable frequency of perivascular cuffing of mononuclear cells (Figure 2C) and glial nodules in the vicinity of the infected area (Table 1). Infected neurons were observed in multiple focal areas (Figure 2D), and sometimes showed intense signals of viral antigen in the cytoplasm, in weak acidophilic inclusion body-like structures, and in neuronal processes.

While milder lung lesions were observed in hamsters infected with rNiV-Fluc^{NP} compared to NiV-M, considering

Table 1. Grading of Histopathological Lesions in Lung and Brain of Syrian Hamster After Exposure to Nipah Virus-Malaysia (NiV-M) Strain and Recombinant Expressing Firefly Luciferase (rNiV-Fluc^{NP})

	Grade			
	NiV-M		rNiV-FLUC	
Lesion	2.0×10^4 PFU (3 hamsters)	1.0×10^5 PFU (2 hamsters)	8.5×10^4 PFU (4 hamsters)	2.0×10^5 PFU (1 hamster)
Lung				
Hyperplasia of type II pneumocytes	3,3,3	3,3	1,3,3,3	3
Multinucleated giant cells	1,3,3	3,3	0,1,1,1	1
Inflammatory cells in alveoli	0,1,2	2,3	0,1,2,3	0
Vasculitis	0,3,3	2,3	0,1,2,3	0
Fibrinous fluid with blood in alveolar space	0,0,0	3,3	0,0,0,0	0
Thrombi formation	0,0,0	1,3	0,0,0,0	0
Edema	0,0,3	1,3	0,0,0,2	0
Brain				
Meningitis	1,2,3	0, 3	0,1,1,1	1
Perivascular cuffing	0,3,3	0,0	0,2,3,3	3
Glial nodules	0,0,0	0,0	0,1,1,1	0
Infected neurons with inclusions bodies	3,3,3	3,3	3,3,3,3	3

Animals chosen for analyses exhibited both respiratory and neurological signs of NiV infection and succumbed to infection between day 6 and 14 postinfection. The severity of the lesions was ranked as: 0, no detectable lesions; 1, rare (1–2 lesions/section); 2, occasional (3–5 lesions/section); 3, frequent (5 or more lesions/section).

Abbreviation: PFU, plaque forming unit.

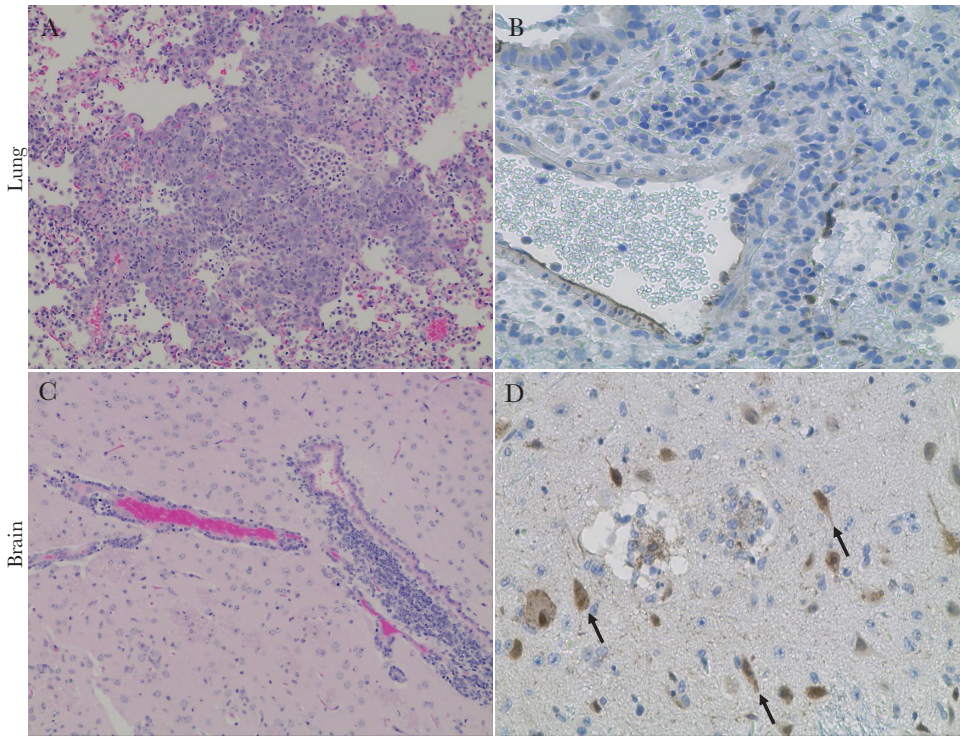

Figure 2. Pathological lesions and viral antigen distribution in the lung and brain of Syrian hamsters following aerosol exposure to Nipah virus Malaysia strain (NiV-M) strain. Hematoxylin and eosin staining (*A, C*) and NiV nucleoprotein staining (brown staining) (*B, D*) of both lung and sagittal brain sections from NiV-M–infected hamsters. Hyperplasia type II pneumocytes with inflammatory cells in alveoli (*A*), NiV-M–infected endothelial cells from large and medium size pulmonary vessels (*B*), severe perivascular cuffing by mononuclear cells in meninges (*C*), and NiV-M–infected neurons (*D*) (arrows). Initial magnification 20 × (*A, C*), 40 × (*B, D*).

the differences in time to death between the animals used for the analysis, it is predicted that lung lesions caused by both viruses are similar. Likewise, our data suggest comparable brains lesions.

In Vivo Imaging of Hamsters After Aerosol Exposure to rNiV-Fluc^{NP}

In order to visualize NiV infection and spread in living animals, a group of 3 hamsters was exposed to aerosolized rNiV-Fluc^{NP} (10^5 PFU) and the virus replication-related bioluminescence was monitored daily, starting day 1 postinfection, using an IVIS Spectrum imager. Aerosol exposure resulted in infection primarily confined to the lungs at day 1 postinfection. The signal was also intensely detected, although delayed, in the oropharyngeal/oronasal area and possibly the brain by day 2 postinfection, with bioluminescence levels in these regions gradually increasing until at least day 5–6 postinfection (Figure 3A, 3B, and Figure 4A, 4B). Regions anatomically consistent with the location of the major salivary glands were also bioluminescent at day 1 postinfection, consistent with previous observations in rNiV-Fluc^{NP}–infected mice by intranasal route [31]. Animals then started losing weight on day 4–5 postinfection, and showed signs of respiratory disease such as labored breathing by day 5 postinfection. The disease uniformly progressed to irregular breathing, lethargy, and in 1 animal nosebleed at day 6 postinfection, the day all 3 animals were euthanized. Interestingly, virus replication stayed productive once the infection was established in the aforementioned organs or anatomical areas, and was never detected in peripheral organs (Figure 3A). This is consistent with infectious virus being isolated from the lungs (about 10^4 PFU/g) but surprisingly, not from the brains (data not shown), although viral antigen was detected in the cortex of at least 1 subject (data not shown). Note that no virus was isolated from sera (possibly because this was below the limit of detection of the assay), which is consistent with the fact that NiV-M spreads rather by peripheral blood mononuclear cell-associated viremia [34]. Only animals exposed to 10^5 PFU of rNiV-Fluc^{NP} from the serial dosing study (Figure 1B), and whose disease evolved until day 10 to 13 postinfection, primarily displayed intense bioluminescence in the brain (Figure 3B) where low levels of infectious virus were isolated (data not shown). This suggests that lower levels of replication in the lung, as seen few days postexposure, and possibly clearance-related, favor a lengthy progression of the disease.

DISCUSSION

The objective of this study was to characterize the pathogenicity of small-droplet aerosols of NiV-M strain in Syrian hamsters,

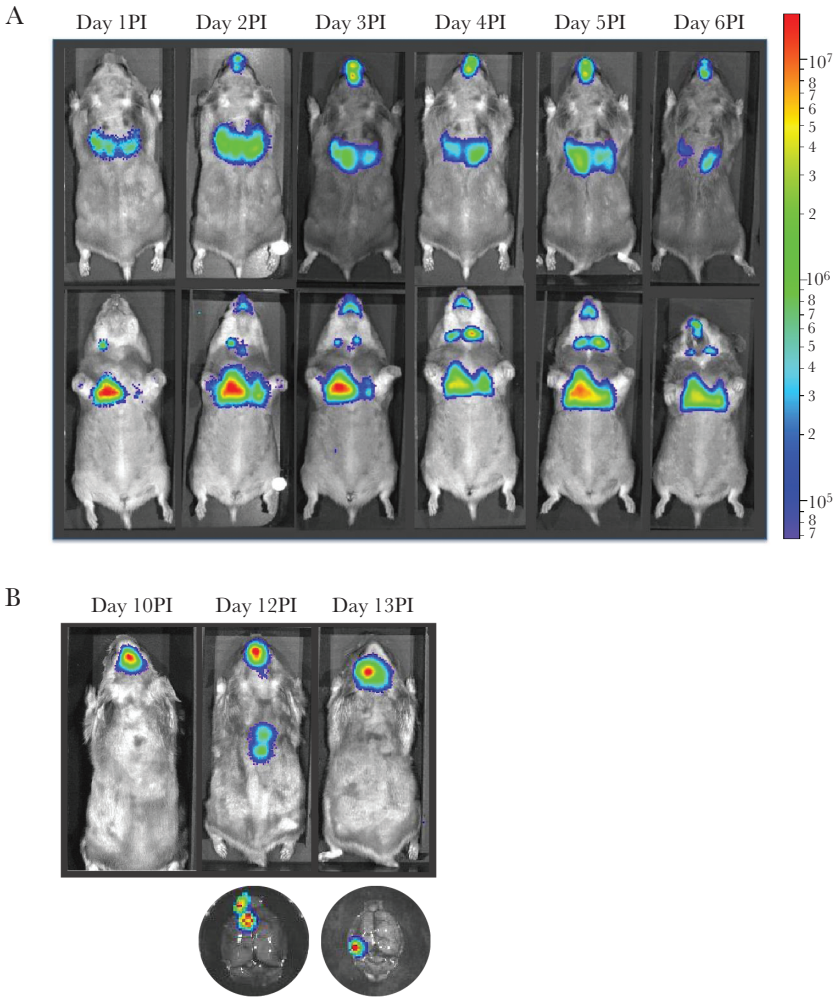

Figure 3. Imaging of recombinant Nipah virus (rNiV-Fluc^{NP}) replication and spread in real time in Syrian hamsters. (*A*) In vivo imaging system (IVIS) of hamsters (n = 3) exposed to aerosolized 10^5 plaque forming units (PFU) of rNiV-Fluc^{NP}. All animals were imaged daily for 6 days and data for 1 representative animal are shown. Top row: dorsal side; bottom row: ventral side. Viral replication can be observed as early as day 1 postinfection (PI) in the lungs and anatomical areas of the lymph nodes, and as early as day 2 postinfection in the region of the olfactory bulb. (*B*) Animals exposed to aerosolized 10^5 PFU of rNiV-Fluc^{NP} from the initial serial dosing study (Figure 1B) that survived beyond day 6 postinfection were imaged at days 10, 12, and 13 postinfection. Brains from animals euthanized at days 12 and 13 postinfection, respectively, were imaged by IVIS immediately after necropsy. Luciferase signals were detected in the brain.

and to follow its spatial and temporal spread in live animals. Although NiV-M is not the most recent circulating strain, NiV-M patients exhibited clinical signs of a respiratory involvement and displayed lung lesions [3] similar to those found in both NiV-Bangladesh (NiV-B)- [35] and NiV-M- [36] infected human lung grafts, and hamsters [15, 25, 37] or other animal models [13, 38]. Therefore NiV-M is as suitable as NiV-B to study NiV respiratory disease even though the latter virus strain is a greater threat due to a well-documented human-to-human dissemination [7–10, 12]. The Syrian hamster was chosen because it is the most characterized rodent models to study NiV pathogenesis [11, 15, 16, 18, 19, 25, 30, 37, 39, 40] and recapitulates the major aspects of clinical disease seen in patients [3, 4, 21, 22].

The main suspected route of NiV-B infection in humans is by consuming NiV-contaminated food and close contact with human body fluids [7, 12, 23, 28], while NiV-M transmission rather occurred following close contact with infected animals [4–6, 24]. Therefore, aerosolized NiV from NiV-contaminated biologics could potentially constitute another relevant mode of transmission. Successful NiV-M infection of nonhuman primates by aerosolized exposure was recently reported [29], even though unassisted aerosol transmission from NiV-infected hamsters and ferrets to naive animals could not be established, regardless of the virus strain [13, 15]. To date, data on NiV aerosol transmission are sparse. Yet, it is critical to determine whether this transmission mode is relevant in order to take appropriate measures to prevent further natural infections. Study of the infectivity of aerosolized henipaviruses is also instrumental in risk assessment of their potential use in agro-biowarfare attack.

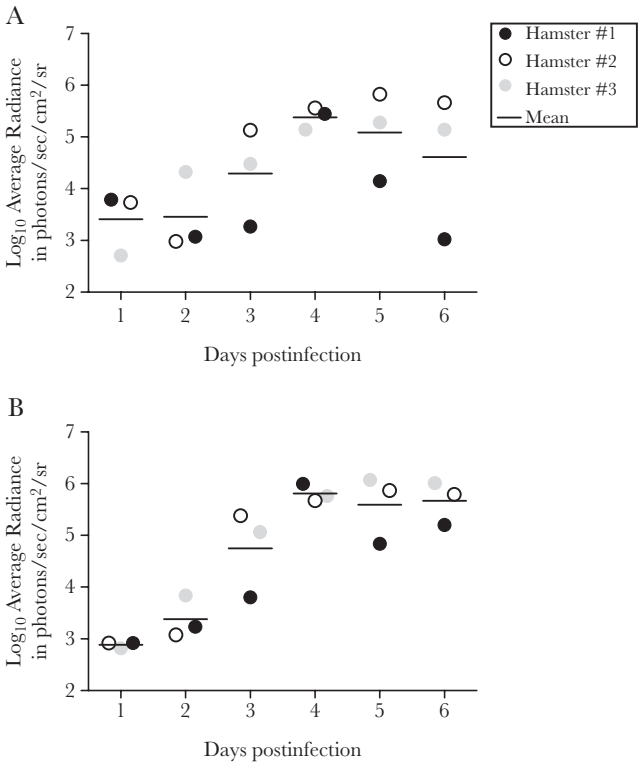

Figure 4. Quantification of radiance of rNiV-Fluc^{NP} spread-related luminescence output in Syrian hamsters. Quantification of average radiance from the (*A*) lung region and (*B*) anatomical region encompassing the olfactory bulb and brain. Measurements from 3 individual animals are indicated by filled and open circles. The average is displayed as a horizontal bar. These graphs are intended to present a trend in increased luminescence signals over time.

Here, the average time to death in hamsters ranged from 7.2 to 13.5 days with about half of animals exhibiting signs of both respiratory disease and neurological involvement, which is in line with similar studies using the AGM model [17, 29, 38]. Note that even though the survival rate was unexpectedly high in our NiV-M 10^4 dose group, the average time to death of the animals (60%) showing clinical manifestations of disease was still in line with those of flanking dose groups. In addition, the median lethal dose and a high infective dose causing uniformly, but not exclusively, respiratory disease prior death were also reported in the hamster model using other routes of infection [15, 19, 30]. Therefore, inhalation of 1 to 2-μm diameter small-particle NiV-M aerosol or of NiV-M liquid inoculum produces equivalent clinical manifestations of the disease in the hamster model. Interestingly, some of the histopathological lesions found in the brain and lung, the 2 major sites of replication, were similar to those found in NiV patients [1, 3, 4, 21, 22]. However, the presence of nodules across the lung was a new pathological feature only previously documented in AGM, also after NiV-M aerosol exposure [29].

We applied IVIS imaging to monitor the temporal spread of the recombinant NiV-M expressing firefly luciferase. Virus replication was primarily initiated in the lungs and to a lesser extent in anatomical areas consistent with the salivary glands starting day 1 postinfection, suggesting that the majority of droplets deposited in the lower respiratory tract. This is consistent with the travel capabilities of the monodisperse aerosols generated in our study [41]. Starting day 2 postinfection, virus was additionally detected in the oral, nasal, or pharyngeal cavity, and is in line with detection of NiV in the olfactory epithelium reported at the same time in the same animal model using the intranasal route [18]. Also, conversely to our previous observation from intraperitoneal NiV-infected mice whose central nervous system (CNS) invasion started at a similar time [31], no bioluminescence signal could be detected from the periphery. Therefore, CNS invasion in hamsters could be occurring predominantly via the olfactory mucosa and olfactory nerves [18, 25, 42] or by other cranial nerves as shown in pigs [42], rather than through systemic spread starting as early as day 2 postinfection after NiV aerosol exposure. It is unclear whether human CNS invasion through cranial nerves is relevant due to differences in anatomy with our rodent models. Note that NiV-M aerosol exposure did not cause a neurological disease in the AGM model [29]. However, we agree with the authors that it was likely due to the severity of the respiratory infection being the major contributory factor to death [29].

In conclusion, our results indicated that aerosolized NiV-M and its derivative rNiV-Fluc^{NP} caused similar clinical manifestations of disease and lesions in lung and brain, the 2 major sites of NiV replication. Our system generated monodisperse aerosols containing virus particles and this mode of infection in the hamster model did not change the course of disease when compared to intranasal inoculation with similar infective doses [15, 19, 25, 30, 37]. Finally, we were able to monitor spread of NiV in hamsters using IVIS imaging, a technology that could be used in future studies evaluating the efficacy of antiviral therapeutics and vaccine candidates.

Notes

Acknowledgment. We thank Igor Patrikeev (Center for Biomedical Engineering, University of Texas Medical Branch) for technical assistance with IVIS imaging.

Financial support. This work was supported by National Institutes of Health (grant numbers R33 AI102267 to A.N.F. and B.L., RO1 AI123449 to B.L., and R21 AI111042 to A.N.F.); and by The University of Texas Medical Branch Department of Pathology start-up funds (to A.N.F.). Aerosol challenges were supported by the Galveston National Laboratory Aerobiology Core Facility.

Potential conflicts of interest. All authors: No reported conflicts of interest. All authors have submitted the ICMJE Form for Disclosure of Potential Conflicts of Interest. Conflicts that

the editors consider relevant to the content of the manuscript have been disclosed.

References

1. Chua KB, Bellini WJ, Rota PA, et al. Nipah virus: a recently emergent deadly paramyxovirus. Science **2000**; 288:1432–5.
2. Eaton BT, Broder CC, Wang LF. Hendra and Nipah viruses: pathogenesis and therapeutics. Curr Mol Med **2005**; 5:805–16.
3. Wong KT, Shieh WJ, Kumar S, et al.; Nipah Virus Pathology Working Group. Nipah virus infection: pathology and pathogenesis of an emerging paramyxoviral zoonosis. Am J Pathol **2002**; 161:2153–67.
4. Chua KB, Lam SK, Goh KJ, et al. The presence of Nipah virus in respiratory secretions and urine of patients during an outbreak of Nipah virus encephalitis in Malaysia. J Infect **2001**; 42:40–3.
5. Goh KJ, Tan CT, Chew NK, et al. Clinical features of Nipah virus encephalitis among pig farmers in Malaysia. N Engl J Med **2000**; 342:1229–35.
6. Paton NI, Leo YS, Zaki SR, et al. Outbreak of Nipah-virus infection among abattoir workers in Singapore. Lancet **1999**; 354:1253–6.
7. Gurley ES, Montgomery JM, Hossain MJ, et al. Person-to-person transmission of Nipah virus in a Bangladeshi community. Emerg Infect Dis **2007**; 13:1031–7.
8. Harit AK, Ichhpujani RL, Gupta S, et al. Nipah/Hendra virus outbreak in Siliguri, West Bengal, India in 2001. Indian J Med Res **2006**; 123:553–60.
9. Hossain MJ, Gurley ES, Montgomery JM, et al. Clinical presentation of Nipah virus infection in Bangladesh. Clin Infect Dis **2008**; 46:977–84.
10. Hsu VP, Hossain MJ, Parashar UD, et al. Nipah virus encephalitis reemergence, Bangladesh. Emerg Infect Dis **2004**; 10:2082–7.
11. Lo MK, Rota PA. The emergence of Nipah virus, a highly pathogenic paramyxovirus. J Clin Virol **2008**; 43:396–400.
12. Tan CT, Tan KS. Nosocomial transmissibility of Nipah virus. J Infect Dis **2001**; 184:1367.
13. Clayton BA, Middleton D, Arkinstall R, Frazer L, Wang LF, Marsh GA. The nature of exposure drives transmission of Nipah viruses from Malaysia and Bangladesh in ferrets. PLoS Negl Trop Dis **2016**; 10:e0004775.
14. Clayton BA, Middleton D, Bergfeld J, et al. Transmission routes for Nipah virus from Malaysia and Bangladesh. Emerg Infect Dis **2012**; 18:1983–93.
15. de Wit E, Bushmaker T, Scott D, Feldmann H, Munster VJ. Nipah virus transmission in a hamster model. PLoS Negl Trop Dis **2011**; 5:e1432.
16. de Wit E, Prescott J, Falzarano D, et al. Foodborne transmission of Nipah virus in Syrian hamsters. PLoS Pathog **2014**; 10:e1004001.
17. Geisbert TW, Daddario-DiCaprio KM, Hickey AC, et al. Development of an acute and highly pathogenic nonhuman primate model of Nipah virus infection. PLoS One **2010**; 5:e10690.
18. Munster VJ, Prescott JB, Bushmaker T, et al. Rapid Nipah virus entry into the central nervous system of hamsters via the olfactory route. Sci Rep **2012**; 2:736.
19. Rockx B, Brining D, Kramer J, et al. Clinical outcome of henipavirus infection in hamsters is determined by the route and dose of infection. J Virol **2011**; 85:7658–71.
20. Chong HT, Kunjapan SR, Thayaparan T, et al. Nipah encephalitis outbreak in Malaysia, clinical features in patients from Seremban. Can J Neurol Sci **2002**; 29:83–7.
21. Chua KB. Nipah virus outbreak in Malaysia. J Clin Virol **2003**; 26:265–75.
22. Chua KB, Goh KJ, Wong KT, et al. Fatal encephalitis due to Nipah virus among pig-farmers in Malaysia. Lancet **1999**; 354:1257–9.
23. Luby SP, Rahman M, Hossain MJ, et al. Foodborne transmission of Nipah virus, Bangladesh. Emerg Infect Dis **2006**; 12:1888–94.
24. Mounts AW, Kaur H, Parashar UD, et al. A cohort study of health care workers to assess nosocomial transmissibility of Nipah virus, Malaysia, 1999. J Infect Dis **2001**; 183:810–3.
25. Baseler L, Scott DP, Saturday G, et al. Identifying early target cells of Nipah virus infection in Syrian hamsters. PLoS Negl Trop Dis **2016**; 10:e0005120.
26. Escaffre O, Borisevich V, Carmical JR, et al. Henipavirus pathogenesis in human respiratory epithelial cells. J Virol **2013**; 87:3284–94.
27. Escaffre O, Borisevich V, Vergara LA, Wen JW, Long D, Rockx B. Characterization of Nipah virus infection in a model of human airway epithelial cells cultured at an air-liquid interface. J Gen Virol **2016**; 97:1077–86.
28. Luby SP, Gurley ES, Hossain MJ. Transmission of human infection with Nipah virus. Clin Infect Dis **2009**; 49:1743–8.
29. Cong Y, Lentz MR, Lara A, et al. Loss in lung volume and changes in the immune response demonstrate disease progression in African green monkeys infected by small-particle aerosol and intratracheal exposure to Nipah virus. PLoS Negl Trop Dis **2017**; 11:e0005532.
30. DeBuysscher BL, de Wit E, Munster VJ, Scott D, Feldmann H, Prescott J. Comparison of the pathogenicity of Nipah virus isolates from Bangladesh and Malaysia in the Syrian hamster. PLoS Negl Trop Dis **2013**; 7:e2024.
31. Yun T, Park A, Hill TE, et al. Efficient reverse genetics reveals genetic determinants of budding and fusogenic differences between Nipah and Hendra viruses and enables real-time monitoring of viral spread in small animal models of henipavirus infection. J Virol **2015**; 89:1242–53.
32. Roy CJ, Pitt LM. Infectious disease aerobiology: aerosol challenge methods. In: Swearengen JR, ed. Biodefense

research methodology and animal models. Boca Raton, FL: CRC Press, **2012**:65–80.
33. Guyton AC. Measurement of the respiratory volumes of laboratory animals. Am J Physiol **1947**; 150:70–7.
34. Johnston SC, Briese T, Bell TM, et al. Detailed analysis of the African green monkey model of Nipah virus disease. PLoS One **2015**; 10:e0117817.
35. Escaffre O, Saito TB, Juelich TL, et al. Contribution of human lung parenchyma and leukocyte influx to oxidative stress and immune system-mediated pathology following nipah virus infection. J Virol **2017**; 91:pii:e00275-17.
36. Valbuena G, Halliday H, Borisevich V, Goez Y, Rockx B. A human lung xenograft mouse model of Nipah virus infection. PLoS Pathog **2014**; 10:e1004063.
37. Baseler L, de Wit E, Scott DP, Munster VJ, Feldmann H. Syrian hamsters (*Mesocricetus auratus*) oronasally inoculated with a Nipah virus isolate from Bangladesh or Malaysia develop similar respiratory tract lesions. Vet Pathol **2015**; 52:38–45.
38. Mire CE, Satterfield BA, Geisbert JB, et al. Pathogenic differences between Nipah virus Bangladesh and Malaysia strains in primates: implications for antibody therapy. Sci Rep **2016**; 6:30916.
39. Walpita P, Cong Y, Jahrling PB, et al. A VLP-based vaccine provides complete protection against Nipah virus challenge following multiple-dose or single-dose vaccination schedules in a hamster model. NPJ Vaccines **2017**; 2:21.
40. Wong KT, Grosjean I, Brisson C, et al. A golden hamster model for human acute Nipah virus infection. Am J Pathol **2003**; 163:2127–37.
41. Tsuda A, Henry FS, Butler JP. Particle transport and deposition: basic physics of particle kinetics. Compr Physiol **2013**; 3:1437–71.
42. Weingartl H, Czub S, Copps J, et al. Invasion of the central nervous system in a porcine host by Nipah virus. J Virol **2005**; 79:7528–34.